ISSN : 0974 - 7486 Volume 8 Issue 4

Trade Science Inc.

Materials Science

An Indian Journal

Full Paper

MSAIJ, 8(4), 2012 [162-168]

Theoretical evaluation of the electrical conductivity variation in $(Bi_2Te_3)_{0.25}(Sb_2Te_3)_{0.75}$ crystallized by THM

G.Kavei*, M.A.Karami

Thermoelectric Lab, Semiconductor Device Fabrication Division, Material and Energy Research Centre (MERC), Tehran, P.O. Box: 4777-14155, (IRAN)

E-mail : g-kavei@merc.ac.ir

Received: 2nd November, 2011 ; Accepted: 2nd December, 2011

ABSTRACT

Experimental and numerical results as presented here demonstrate the adverse effects of a Travelling Heater Method (THM) in $(Bi_2Te_3)_{0.25}(Sb_2Te_3)_{0.75}$ thermoelectric crystallization, on mass transport. Growth with THM reveals that there is a considerable effect from the deflection of the solid–liquid interface, whereas the Bi_2Te_3 stoichiometry does change significantly. At defined length measurements of the thermoelectric crystallized ingot, electrical conductivity was carried out at intervals of defined length (6mm). A sensible gradient was observed in the reading along the ingot from a fulfilled tip to the end. To understand this variation by taking into account all practical experiences of a crystal growth, we must conduct a numerical study because it gives vast information on a crystal growing process. Simulating the crystallization process and characterization of the ingots disclose a variation in the measured values of the thermoelectric parameters which was attributed to the deviation of Bi2Te3 concentration along the ingot.

KEYWORDS

Zone melting method or Travelling Heater Method (THM);
X-Ray Diffraction (XRD and X-Ray Fluorescence (XRF).

INTRODUCTION

Almost all electronic and optoelectronic devices need semiconductor singly crystallized materials. These semiconductor materials are produced through a controlled solidifying process called crystallization growth. Today, most bulk semiconductors are grown from a liquid phase through growth processes known as melt/solution techniques.

The Travelling Heater Method (THM) falls into a category of solution growth, and it is a relatively promising technique for commercial production of bulk compound and alloy semiconductors. Thanks to its importance, a number of experimental and theoretical studies have been made on the THM growth process[1, 2]. This method serves as a main utility for the scientists who have to handle the thermoelectric samples as a crystal. Consequently, numerous studies were made on what constitutes the base of a THM[3-5]. In one of the earliest investigations, the steady-state temperature profiles within the growth ampoule of CdTe to be used for various heater positions were provided[6]. In this topic a series of experiments under an introduced forced-convection by using an accelerated rotation technique were

also studied. THM growth of PbTe and examination of the gravity effect on heat and mass transfer in the liquid zone has been mathematically modelled[7]. THM growth of PbTe has also been studied by a simple mathematical model by which the influence of a thermal diffusion effect in this system was examined as a Soret effect[8]. A numerical modelling study and a uni-dimensional numerical simulation for the growth of $Ga_xIn_{1-x}As$ were subjects for discussion in[9]. Finite element, quasi steady-state thermal model for the simulating of HgCdTe growth was used by[10], where transients in the temperature field caused by the displacement of the ampoule in the furnace were not born in mind, and the solvent/crystal interfaces were assumed to be set at the equilibrium liquidus temperature. The influence of thermosolutal convection, though were missed the mark of CdTe growth[10], but was considered after a quasisteady-state model was adopted[11]. In their finite element simulation model, a fixed length of liquid zone was adopted. In order to understand better the complex transport phenomena including the diffusion and convection of heat and mass transfer during the growth processes of ternary alloys[12], have introduced a mathematical model for the growth of GaxIn1-xSb by THM. For numerical simulations of the THM growth process, an adaptive finite element technique was employed. Comparisons with experiments are also provided to assess the validity of the model and computations. Numerical studies on the THM growth of HgTe by using a three-step computational scheme to minimize the computational demand were also undertaken by[13]. The field equations were solved by using a quasisteady-state approximation. Also, the growth conditions that lead to solvent inclusions into the grown crystal were examined. Numerical simulation study for the THM growth of GaSb from a Ga-solution has been conducted by[14], where the effects of crucible temperature, crucible rotation, and crucible material on the crystal/solution interface shape were examined. In order to minimize the adverse effect of convection, which may adversely affect the quality of the grown crystals, and also to obtain a better mixing in the liquid solution, some applied magnetic fields have been used in THM, (see for instance[15-17]). The effect of a rotating magnetic field on the radial compositional uniformity in CdHgTe crystals grown by THM was also examined[18]. The two-dimensional numerical simulation of the THM growth of CdTe focused on the influence of rotating magnetic fields on flow patterns and compositional uniformity in the solution was expressed by[19]. It was found that under microgravity conditions, any applied position of rotating magnetic fields can suppress the residual buoyancy convection in the solution, and may result in complex flow structures and enhanced compositional nonuniformity at high gravity levels. Two-dimensional numerical simulations for the growth of CdTe by THM to test the effect of applied stationary and rotating magnetic fields, as well as that of small nonuniformities in the strong stationary magnetic field were well considered in[20]. Three dimensional simulations for the THM growth process have been carried out by[21] under static but strong applied magnetic fields. Also carried out in[22] is a numerical simulation of Czochralski crystal growth under the influence of a travelling magnetic field as generated by an internal heater-magnet module.

All attempts in these studies are to consider the THM performance employed for crystallization growth and approach, in reality, to its adverse effect on the thermoelectric parameters in particular the electrical conductivity by using a numerical simulated method. In fact, it was reported by Kasap[23] and Sze that[24], multi-element e.g. ternary compounds with defined stoichiometry that was intended to be crystallised by THM provides such intrinsic effect by means of a phase diagram system.

The aim this study is to consider the THM performance which frequently available for crystal growth and approach, its adverse effects on the thermoelectric parameters in particular the electrical conductivity by using a numerical simulated method.

EXPERIMENT

THM stands for a solution growth technique that can be used for growing and synthesizing binary and ternary compound semiconductors. In THM, growth of $(Bi_2Te_3)_{0.25}(Sb_2Te_3)_{0.75}$ thermoelectric semiconductor single crystals is kept molten by a narrow heater. As the heater's gauge moves upward, 50% solid solution of an alloy of feed source type is dissolved at the melting interface and 50% of compound is deposited at the solidus interface.

Full Paper

This process allows a constantly controlled but slow growth to be made possible. The quality of grown crystals in THM is very sensitive to the relative variation of temperature profile by which a growth rate is determined. THM has a number of advantages over melt techniques the most notable of which are less thermal stresses, growth of ternary alloys, and uniform crystal composition.

The experimental procedures that are applied to provide thermoelectric samples were described in previous publications[25-26]. The aim of this research is to analyze the processes of a crystal growth by THM and know how it adversely effects it has on the thermoelectric parameters in particular the electrical conductivity. It is believed that some modification should be usefully made to overcome the problem. In fact, as reported by Kasap[23], and Sze[24], when multi-element compound with a well-defined stoichiometry were to be crystallized by THM, violation of a crystal ingot stoichiometry would be inevitable. Dissimilar mobility, solidification of the elements on a pre-selected temperature, a rate of crystallization and an intrinsic behavior of the phase diagram is accounted for it.

Crystal growth

Figure 1(a) shows a schematic view of a HTM furnace that is used for the growth of $(Bi_2Te_3)_{0.25}(Sb_2Te_3)_{0.75}$, a simple heater moves up by means of a gear box system attached to it. Figure 1(b) illustrates the concentration of Bi_2Te_3 in various section of ingot during the crystallization as a function of *y*. Figure 1(c) shows an initial temperature profile of a heater. The growth furnace, consists of three temperature zones all of which can be controlled independently. $(Bi_2Te_3)_{0.25}(Sb_2Te_3)_{0.75}$ filled into an ampoule evacuated at 10^{-6} Torr and sealed as synthesized in the furnace. The temperature of the furnace was controlled between 650 and700 °C. This is due to Bi_2Te_3 and Sb_2Te_3 melting point at about 650 °C and 10^{-3} Torr. The cooling rate throughout the crystal growth was about 0.61°C.h^{-1}.

Numerical study

Due to the height limitation of the THM heater (5mm), it could not easily read the temperature distribution of the heater from its tip to end. Numerical method

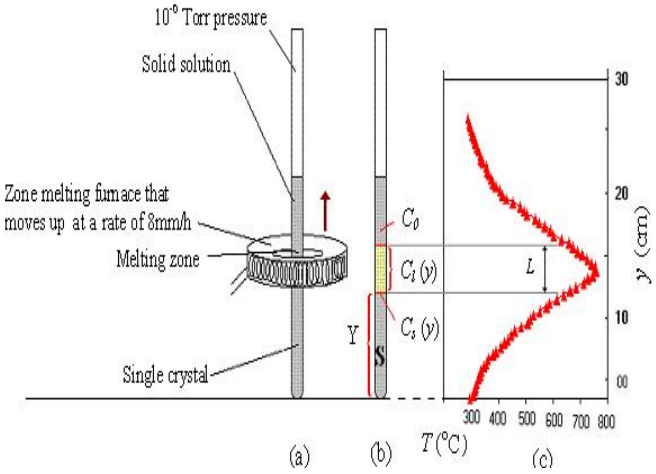

Figure 1(a) : Schematic view of travelling heater, (b) Concentration of Bi_2Te_3 in various section of ingot during the crystallization as function of *y*, (c) Thermal distribution function around melting region.

was a suitable one to deal with the problem. Consequently, the temperature distribution on the heater which was computed by way of a two-dimensional conductive heat transfer simulation method as shown in Figure 1c can be defined. Temperatures for individual regions from centre to edge of the heater were used as input, while the effect of convection was neglected.

However, along the heater as the heat insulation of THM system was ineffective high temperature gradient was developed and sensible convection in the liquid zone adversely affected the quality of grown crystals. As reported by[15-16], the application of an external stationary magnetic field is an option to suppress the convective flow in the liquid zone. The field, as were in perfectly line with the axis of a growth cell, creates a magnetic body force in a horizontal plane which in turn balances a vertical gravitational body force, and consequently suppresses the convective flow and brings about a different motivation amongst constituent elements in ternary compounds. Nevertheless, the presence of Bismuth in the thermoelectric samples acts as a barrier to use a field.

Figure 3 showed the temperature profile for the heater, the tube and the compound when they reach a thermal and a chemical quasisteady-state equilibrium within the ampoule, considering the fact that the ampoule moves downward largely depending on the heater that has a very small displacement velocity usually for the present work in the order of 8 mm per hour. Over the growth process, a temperature difference between

the upper (dissolution) and the lower (growth) liquid-solid interfaces appeared. This is due to the asymmetrical thermal profile with its higher temperature at the dissolution interface. The source material is thereby dissolved at the upper interface, where its solubility increases due to the heater movement. The material is transported through the liquid zone by both thermosolutal convection and diffusion. Recrystallization then occurs at the lower interface, the temperature of which is lower than that of the dissolution interface. In essence, the heater thermal gradient (temperature profile) and its movement are two important factors that can control the growing process. The temperature gradient in the vicinity of the growth interface must be properly controlled so as to avoid constitutional super cooling and thermal stresses. This can be achieved by an optimum thermal design for the THM growth crucible.

RESULTS AND DISCUSSION

Simulation

Bi_2Te_3 and Sb_2Te_3 are completely soluble in a consistently solid solution as illustrated in the phase diagrams in Figure 2[27]. The solid solution that corresponds to each point of phase diagram varies in compound but not in crystal structure from pure Sb_2Te_3 to pure Bi_2Te_3, which must necessarily have the same structure[23]. The lattice parameters of solid solution also vary all through a pure Sb_2Te_3 to a pure Bi_2Te_3.

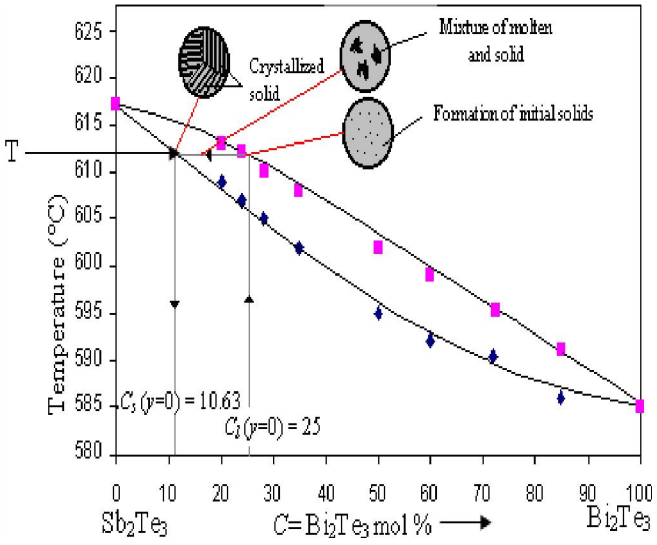

Figure 2 : Quasi phase ternary diagram of Sb_2Te_3- Bi_2Te_3 system[26b].

Homogenous ingot of $(Bi_2Te_3)_{0.25}(Sb_2Te_3)_{0.75}$ was prepared by co-melting of Bi, Te and Sb elements. Refereeing to Figure 2, which is a quasi phase ternary diagram of Sb_2Te_3-Bi_2Te_3 system. In this diagram the formation of a $(Bi_2Te_3)_{0.25}(Sb_2Te_3)_{0.75}$ at 611°C, C_s=10.63 and $C_o = C_l = 25$ will take place, are both the concentration of Bi_2Te_3 at the points of crystallization and the formation of the solidus respectively. A glance at a staring crystallizing process shall make us understand that the heater temperature should be at 611°C. At the starting point of the growth operation, heater moves up at a small fraction (8mm/hour) and the discrepancy of the C_s and C_l will appear. As the heater moves upward, a rapid and sensible temperature decrement would be inevitable at S region in the Figure 1, due to exiting the molten region from the heat source boundary. Therefore, as the quasi phase diagram shows the concentration at the solid and liquid boundary $C_S = 10.63$ cannot be aligned with the equilibrium value of $C_o = C_l = 25$. Thus, the solid solution at (*S*) has a lower concentration rate of Bi_2Te_3 than that included at (l). Since the heater continues to move up the concentration discrepancy, $(C_l - C_S)$ has been pushed out of the freezing region to the molten zone.

As the heater moves up by d*y*, the molten zone is also pushed up. Therefore, the solid concentration that enters the molten zone from the upper region of the ingot is $\frac{\mathbf{C_o dy}}{\mathbf{L}}$. Meanwhile, the solidus concentration which leaves the molten zone is $\frac{\mathbf{C_s(y)dy}}{\mathbf{L}}$ [20]. Thus, the Bi_2Te_3 concentration in molten zone will be:

$$\mathbf{dC_l(y) = \frac{(C_o - C_s(y))dy}{L}} \qquad (1)$$

where $C_l(y)$ is a liquidus concentration at melted region and L is a molten zone height in constant (~5mm). Integration of Equation1 leads to:

$$\frac{1}{L}\int_0^y dy = \int_{C_0=25}^{C_l(y)} \frac{dC_l(y)}{C_0 - C_s(y)} \qquad (2)$$

To solve this integration, $C_S(y)$ must be derived as a function of $C_l(y)$. Using the least square method[28], two curves are fitted to the experimental data of phase diagram. Figure 2 shows that there are quadratic polynomial relations between both $T_l(C)$ and $C_l(y)$, as well

Full Paper

as an additional $T_S(C)$ and $C_S(y)$ as detailed below:

$$T_l(C) = aC_l^2(y) + bC_l(y) + d = -0.0019C_l^2(y) - 0.1187C_l(y) + 616.67$$
$$T_s(C) = a'C_s^2(y) + b'C_s(y) + d' = 0.0005C_s^2(y) - 0.35C_s(y) + 616.18 \quad (3)$$

where the coefficients α, b, c, α′, c′ and d′ are constant.

For a defined temperature *T*,(see Figure 2), the relation for $C_S(y)$ and $C_l(y)$ can be obtained as below:

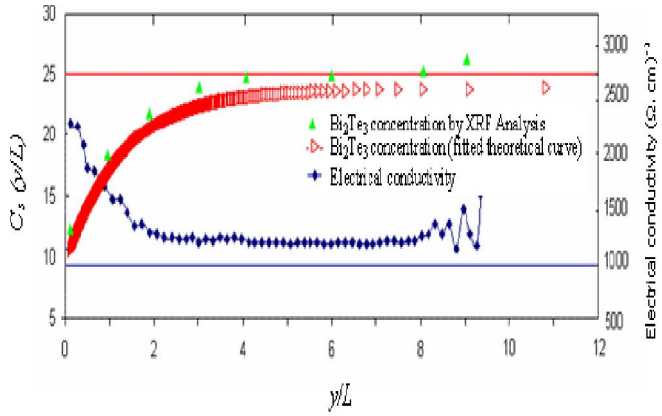

Figure 3(a) : C_l **(*y*/*L*) concentration of Bi_2Te_3 in melting zone as a function of *y*/*L*, (b)** C_s **(*y*/*L*) concentration of Bi_2Te_3 in grown ingot as a function of *y*/*L*.**

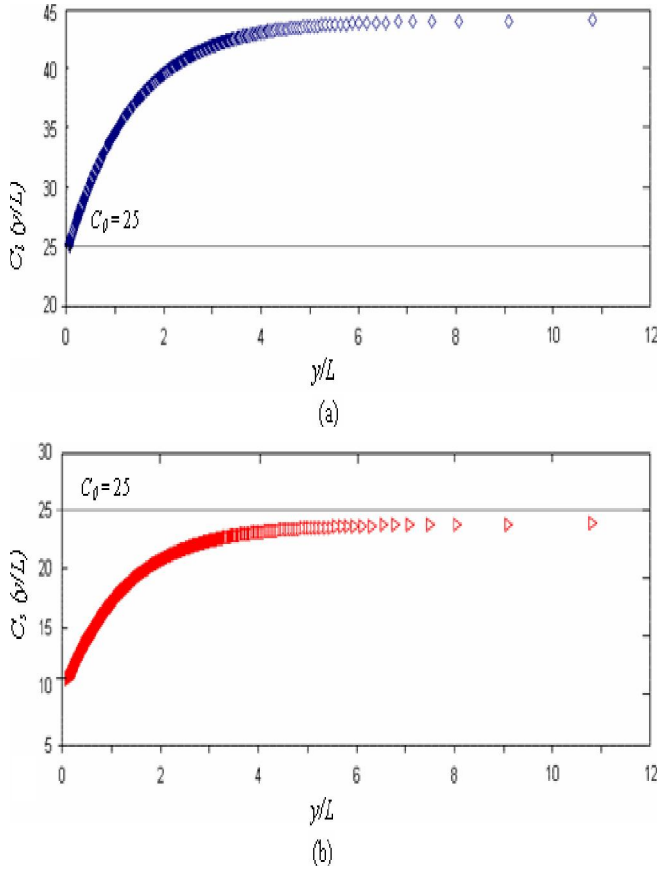

Figure 4 : Electrical conductivity and variation of Bi_2Te_3 concentration as a function of *y*/*L*.

$$T_l(C) = T_s(C)$$
$$aC_l^2(y) + bC_l(y) + d = a'C_s^2(y) + b'C_s(y) + d'$$
$$C_s(y) = \frac{-b' \pm \sqrt{b'^2 - 4a'(d' - (aC_l^2(y) + bC_l(y) + d))}}{2a'} \quad (4)$$

Substituting $C_S(y)$ from Equation 4 for Equation 2:

$$\frac{y}{L} = \int_{C_0=25}^{C_l(y)} \frac{dC_l(y)}{C_0 - \frac{-b' \pm \sqrt{b'^2 - 4a'(d' - (aC_l^2(y) + bC_l(y) + d))}}{2a'}} \quad (5)$$

In Equation 5, since $C_l(y)$ is an upper limit and an integration variable altogether, the integral equation cannot be integrated directly. Therefore, it can be solved numerically as ranges from $C_l(y) = 25$ to $C_l(y) = 45$, (see Figure 2).

Figure 3a shows the result of this integration that presents the variation of $C_l(y)$ vs. $\frac{y}{L}$. With $C_l(y)$, $C_S(y)$, as a concentration factors of Bi_2Te_3 in an crystallized ingot, can be calculated from Equation 1 as a function of $\frac{y}{L}$. Figure 3b shows the variation of $C_S(y)$ vs. $\frac{y}{L}$. It can be seen that for the first quarter length of the ingot, the concentration degree of Bi_2Te_3, $C_S(y)$ is less than C_o but it increases along the course of ingot (with $\frac{y}{L}$). For sections beyond the first quarter, $C_S(y)$ varies and become equal to its equilibrium value $C_o = C_l$.

Figure 3 shows the variation rate of electrical conductivity along the crystal growth direction. The Figure that validates the electrical conductivity also varies in the first quarter length of the ingot and remains constant elsewhere. The variation of $C_S(y)$ along the crystal growth direction was obtained through numerical modeling and empirically measured by XRF as shown in this Figure 3 It can be seen that they are agree well to each other.

Measurements

In addition electrical conductivity, measurements along the crystallized ingot, that reveals very sensitive variation. X-ray diffraction (XRD) and XRF systems were employed to characterize the structure and composition of the continuous sections of ingot, respectively. The lattice parameter variations with x (Bi_2Te_3 concentration) are shown in Figure 5. The lattice parameter increases almost linearly with x contents according to Vegards' law[21]. Substituting Sb atoms for Bi atoms in

Sb_2Te_3 structure leads to an expanded lattice volume that can triggers XRD diffraction lines to shift toward smaller angles. Typical XRD pattern of crystals from mid section of a grown ingot is shown in Figure 6.

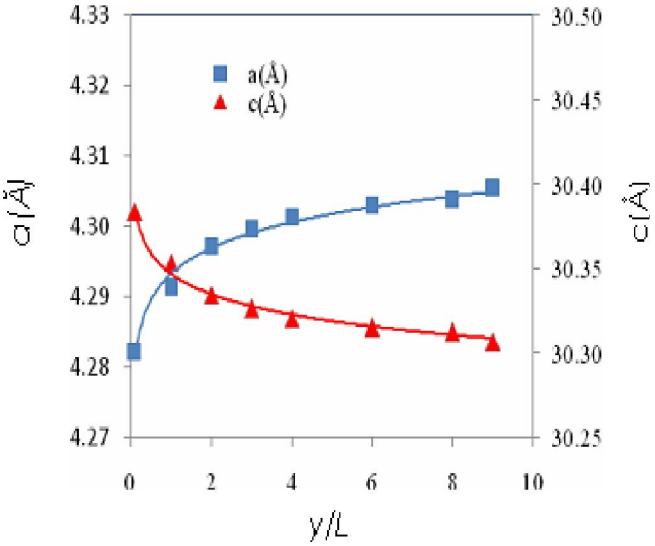

Figure 5 : Variation of the crystal lattice parameters on the composition of solid solution with in Sb_2Te_3- Bi_2Te_3 system.

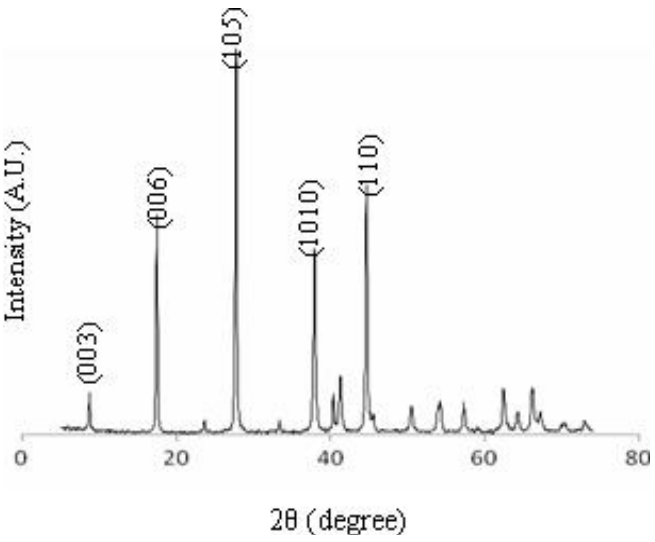

Figure 6 : The XRD pattern of powdered crystals from mid section of a grown ingot.vanna.

CONCLUSION

$(Bi_2Te_3)_{0.25}(Sb_2Te_3)_{0.75}$ thermoelectric semiconductor single crystals were grown by THM. It has been observed that there is a sensible electrical conductivity gradient in the first quarter length of the prepared crystalline ingot. The theoretical and experimental implications showed that the concentration of Bi_2Te_3 along at least the first quarter section of the crystallized ingot is less than its equilibrium value $C_o = 25$ but above this region this value approaches to its equilibrium value. This variation was simulated theoretically and confirmed by the way of XRF and XRD measurements. Variation of Bi_2Te_3 concentration was then found to be responsible for electrical conductivity gradient.

REFERENCES

[1] G.Bischopink, K.W.Benz; J.Crystal Growth, **128**, 466 **(1993)**.

[2] A.N.Danilewski, P.Dold, K.W.Benz; J.Crystal Growth, **121**, 305-314 **(1992)**.

[3] E.Koukharenko, N.Frety, V.G.Shepelevich, J.C.Tedenac; Journal of Alloys and Compounds, **299**, 254-257 **(2000)**.

[4] O.B.Sokolov, S.Ya.Skipidarov, N.I.Duvankovi; Journal of Crystal Growth, **236**, 181-190 **(2002)**.

[5] M.H.Ettenberg, J.R.Maddux, P.J.Taylor, W.A. F. D.Jesser, F.D.Rosi; J.Crystal Growth, **179**, 495 **(1997)**.

[6] F.V.Wald, R.O.Bell; J.Crystal Growth, **30**, 29 **(1975)**.

[7] T.A.Cherepanova, V.N.Kuzovkov; Journal of Crystal Growth, **65(1-3)**, 55-58 **(1983)**.

[8] T.Boeck, P.Rudolph; J.Crystal Growth, **79**, 105-109 **(1986)**.

[9] H.E.Sell, G.Muller; J.Crystal Growth, **97**, 194 **(1989)**.

[10] C.J.Chang, B.Baird, P.K.Liao, R.Chang, L.Colombo; J.Crystal Growth, **98**, 595 **(1989)**.

[11] X.Ye, B.Tabarrok, D.Walsh; J.Crystal Growth, **169**, 704 **(1996)**.

[12] R.A.Meric, S.Dost, B.Lent, R.F.Redden; Int.J.Appl.Electromagnetics Mechanics, **10(6)**, 5056 **(1999)**.

[13] M.C.Martinez-Tomas, V.Munos-Sanjose, C.Reig; J.Crystal Growth, **243**, 463-475 **(2002)**.

[14] Y.Okano, H.Kondo, W.Kishimoto, L.Li, S.Dost; J.Crystal Growth, **237-239**, 1716 **(2002)**.

[15] S.Dost, Y.Liu, B.Lent; 16eme Congres Francais de Mecanique Nice, 1-5 septembre, 1-6 **(2003)**.

[16] L.Abidi, M.Z.Saghir, D.Labrie; Int.J.Materials and Product Tech., **22(1/2/3)**, 2-19 **(2005)**.

[17] V.Kumar, S.Dost, F.Durst; Applied Mathematical Modelling, **31(3)**, 589-605 **(2007)**.

Full Paper

[18] A.S.Senchenkov, I.V.Barmin, A.S.Tomson, V.V.Krapukhin; J.Crystal Growth, **197**, 552 **(1999)**.
[19] C.K.Ghaddar, C.K.Lee, S.Motakef, D.C.Gillies; J.Crystal Growth, **205**, 97 **(1999)**.
[20] S.Dost, Y.C.Liu, B.Lent, R.F.Redden; Int.J.Appl.Electromagnetics & Mechanics, **17(4)**, 271 **(2003)**.
[21] Y.C.Liu, S.Dost, B.Lent, R.F.Redden; J.Crystal Growth, **254**, 285 **(2003)**.
[22] O.Kleina, C.Lechnera, Pierre-E Tienne Drueta, P.P.Jurgen prekelsa, C.Frank-Rotschb, F.M.KieXlingb, W.Millerb, U.Rehseb, P.Rudolphb; Journal of Crystal Growth, **310**, 1523-1532 **(2008)**.
[23] S.O.Kasap; Principle of Electronic Materials and Devices, Mc Grow Hill, Chapter 1, **(2002)**.
[24] S.M.Sze; Semiconductor Devices; Physics and Technology, John Wiley & Sons Inc., Chapter 8, **(2002)**.
[25] G.Kavei, A.A.Khashachi; Journal of Thermoelectricity, **3**, 40-45 **(2005)**.
[26] G.Kavei, and A.M.Karami; Bull.Mater.Sci., **29(7)**, 659-663 **(2006)**.
[27] (a) ASM Alloy Phase Diagrams Center, 2007, T.Caillat et.al.; J.Phys.Chem.Solids, **53**, 227-232 **(1992)**; **(b)** M.J.Smith, R.J.Knight, C.W.Spencer; J. Of Appl.Phys., **33(7)**, 2186-90 **(1962)**.
[28] J.Wolberg; Data Analysis Using the Method of Least Squares-Extracting the Most Information from Experiments, Springer, Germany, **(2005)**.